frontiers | Frontiers in Materials

TYPE Original Research
PUBLISHED 19 June 2025
DOI 10.3389/fmats.2025.1619133

OPEN ACCESS

EDITED BY
Vinod Ayyappan,
King Mongkut's University of Technology North Bangkok, Thailand

REVIEWED BY
Yashas Gowda T. G.,
Malnad College of Engineering, India
Oumaima Bili,
UH2C, Morocco

*CORRESPONDENCE
Luo Fei,
luofei@huhst.edu.cn
Wen Jin,
2959@huhst.edu.cn

RECEIVED 27 April 2025
ACCEPTED 05 June 2025
PUBLISHED 19 June 2025

CITATION
Lingcong M, Fengyu M, Yajuan W, Ying P, Fei L and Jin W (2025) Revisiting polymer crystallization kinetics: experimental validation of the Mo equation for modified PET systems. *Front. Mater.* 12:1619133.
doi: 10.3389/fmats.2025.1619133

Revisiting polymer crystallization kinetics: experimental validation of the Mo equation for modified PET systems

Ma Lingcong[1], Mao Fengyu[1], Wu Yajuan[2], Peng Ying[1], Luo Fei[1]* and Wen Jin[1]*

[1]Hunan Provincial Key Laboratory of Fine Ceramics and Powder Materials, Hunan Provincial Modern Industry School of Advanced Ceramics, Hunan University of Humanities Science and Technology, Loudi, China, [2]Dofuoduo New Materials Co., Ltd., Jiaozuo, Henan, China

This study investigated the non—isothermal crystallization kinetics of pure poly(ethylene terephthalate) (PET) and chain—extended modified PET using DSC at various cooling rates. Through comparing Avrami, Ozawa, and Mo methods, the Mo method was found most effective in describing non—isothermal crystallization. The kinetic parameter F(T) indicated that pure PET crystallized faster than modified PET due to reduced chain mobility in the latter. A positive correlation between F(T) and relative crystallinity was established, showing higher cooling rates accelerate crystallinity development. The E44—modified PET had minimal impact on crystallization kinetics, making E44 a promising modifier. These findings advance the understanding of PET crystallization, and the Mo method serves as a robust framework for related studies, promoting polymer kinetics and opening new avenues for material innovation.

KEYWORDS

non-isothermal crystallization kinetics, PET, Mo method, Avrami equation, Ozawa equation

1 Introduction

As a prominent thermoplastic engineering polymer, polyethylene terephthalate (PET) has achieved widespread industrial adoption due to its exceptional balance of optical transparency, mechanical strength, electrical insulation, and chemical resistance (Billon, 2022; Sangroniz et al., 2020). This saturated polyester, sharing structural similarities with polybutylene terephthalate (PBT), derives its superior properties from a molecular architecture featuring aromatic benzene rings connected by flexible ethylene glycol segments. However, these rigid aromatic components simultaneously impose significant constraints on molecular chain mobility, leading to inherent limitations including sluggish crystallization kinetics, prolonged processing cycles, and suboptimal ultimate crystallinity (Tang and Xin, 2009). Historically developed as a synthetic fiber material, PET underwent a transformative phase in the 1980s when researchers pioneered crystallization enhancement strategies through nucleating agents and crystallization promoters (Cruz-Delgado et al., 2014). Subsequent decades witnessed remarkable advancements in crystallization modification technologies, expanding PET's applications beyond fibrous materials. The polymer's unique combination of molecular polarity, dense chain packing, and high glass transition temperature (Tg ≈ 75°C) has positioned it as a promising candidate

for barrier applications (Ke et al., 2007). Nevertheless, critical challenges persist in oxygen barrier performance, particularly for demanding applications like carbonated beverage and beer packaging, where permeability requirements are exceptionally stringent (Lewis et al., 2003; Qureshi et al., 2000; Sekelik et al., 1999). Crystallinity modulation has emerged as a viable strategy for barrier enhancement, as the impermeable crystalline domains can effectively elongate gas diffusion pathways through tortuosity effects (Calcagno et al., 2007). While conventional thermal annealing can improve barrier properties by perfecting crystal lamellae, this approach often compromises optical clarity and induces embrittlement (Flores et al., 2008). Recent innovations have focused on nanoscale modifications, particularly through the incorporation of layered silicates that create intricate permeation barriers by forcing diffusing molecules to navigate around impermeable platelet structures (Frounchi and Dourbash, 2009; Ke and Yongping, 2005) These nanocomposite systems typically demonstrate 30%–50% reduction in oxygen transmission rates while maintaining acceptable transparency. The crystallization behavior of PET has been extensively characterized through both fundamental studies (Chaari et al., 2003; Gaonkar et al., 2023; Bian et al., 2003; Hanley et al., 2006; Liangbin et al., 2001; Androsch and Wunderlich, 2005; Lu and Hay, 2001; Tan et al., 2000; Piccarolo et al., 2000; Wang et al., 2000; Dupaix and Krishnan, 2006) and nanocomposite investigations (Saujanya et al., 2003; Zheng and Wu, 2007; Wu and Ke, 2007; Wan et al., 2004; Ou et al., 2003). Isothermal crystallization kinetics typically reveal a biphasic mechanism: an initial stage dominated by heterogeneous nucleation and three-dimensional spherulitic growth (Avrami exponent n ≈ 3), followed by secondary crystallization featuring one-dimensional interlamellar growth (n ≈ 1). Nanoparticle incorporation generally reduces half-crystallization time (t1/2) by 20%–40% through heterogeneous nucleation effects, though paradoxical retardation has been reported in certain systems. The controversial impact on equilibrium melting point (Tm°) - with reports showing both increases and decreases (Chen et al., 2007) - suggests complex nanoparticle-polymer interactions that may alter fold surface free energy or chain mobility.

This investigation employs advanced calorimetric analysis (DSC-60) to elucidate the crystallization kinetics of epoxy resin-modified PET systems. Through comprehensive modeling of both isothermal and non-isothermal crystallization data, we aim to establish structure-property relationships between chain-extended architectures, nucleation mechanisms, and crystallization rates. The findings are expected to provide fundamental insights for designing high-performance PET materials with tailored crystallization characteristics and optimized barrier properties.

2 Materials and methods

2.1 Raw materials and sample preparation

Recycled polyethylene terephthalate (R-PET, intrinsic viscosity 0.72 dL/g) was provided by Yangzhou Gaohai Plastic Chemical Fiber Co., Ltd. (China). Industrial-grade epoxy resin (EP, diglycidyl ether of bisphenol A, epoxy equivalent weight 189 g/eq) was supplied by Dasen Material Technology Co., Ltd. (China). The R-PET matrix was modified through reactive chain extension using EP as a chain extender at four different mass fractions (12%, 20%, 44%, and 51%). The resulting modified PET samples were systematically designated as EP-12, EP-20, EP-44, and EP-51, respectively, based on their EP content (Table 1). All materials were vacuum-dried at 120°C for 12 h prior to processing to minimize moisture-induced degradation.

TABLE 1 Experiment formula.

Formula	Mass fraction of chain extender
EP-51(W%)	1.0
EP-44(W%)	1.5
EP-20(W%)	2.1
EP-12(W%)	2.5

Note: The amount of R-PET, added in the above 4 formulations is 60 g.

TABLE 2 Intrinsic viscosity of PET modified by EP chain extender.

Example	ηsp (dL/g)	ηr (dL/g)	[η](dL/g)
1.6% EP1	0.250	0.250	0.250
1.3% EP1	1.250	1.250	1.250
1% EP1	0.926	0.926	0.926
0.7% EP1	0.265	0.265	0.265
1% EP2	0.236	0.236	0.236
0.7% EP3	0.231	0.231	0.231
PET	0.262	0.262	0.262
PET-10min	0.205	0.205	0.205

The materials underwent high - temperature drying followed by cooling to room temperature. Subsequently, the moisture content was measured using a Shimadzu - MOC - 120H moisture meter, and it was effectively controlled below 50 ppm. Afterwards, chain mixing and extension were carried out using a torque rheometer (Model XSS - 300, manufactured by Shanghai Kechuang Rubber and Plastic Machinery Equipment Co., Ltd.). The process was performed at a rotational speed of 60 rpm for a mixing time of 10 min, as presented in Table 2.

2.2 Instrumentation

The experimental setup included: an electronic balance (FA/JA series, ±0.1 mg accuracy, Shanghai Precision Scientific Instrument Co., Ltd.) for precise mass measurement; a vacuum drying oven (DZ-2BC, Tianjin Test Instrument Co., Ltd.) for material pretreatment; a torque rheometer (XSS-300, Shanghai

Kechuang Rubber and Plastic Machinery Equipment Co., Ltd.) equipped with twin conical rotors for melt processing; and a differential scanning calorimeter (DSC-60, Shimadzu Corporation, Japan) with ±0.1°C temperature accuracy for thermal analysis.

2.3 Thermal analysis protocol

Thermal characterization was performed using the DSC-60 analyzer under nitrogen purge (30–50 mL/min). For non-isothermal crystallization studies, samples (6–8 mg) were first heated from ambient temperature to 280°C at 99°C/min (held for 5 min to erase thermal history), then cooled to 50°C at controlled rates (5, 10, 15, and 20°C/min) while recording exothermic peaks. Isothermal crystallization experiments involved: (1) initial heating to 280°C (99°C/min, 5 min hold), (2) rapid quenching to 190°C (99°C/min) for isothermal crystallization over 30 min, and (3) subsequent heating to 280°C at 2°C/min to record melting behavior. Three replicates were performed for each condition to ensure data reproducibility.

3 Results and discussion

3.1 Isothermal crystallization behavior analysis

The thermal behavior of chain-extended modified PET was systematically investigated through differential scanning calorimetry (DSC). Figure 1 presents the DSC thermograms obtained after eliminating thermal history, isothermal crystallization at 190°C, and subsequent heating. Comparative analysis reveals a distinct low-temperature shift in the melting endotherm of modified PET relative to unmodified PET, suggesting a reduction in chain regularity induced by the chain extension modification. As quantified in Table 3, the melting point depression (ΔT_m) between modified and pure PET specimens was observed to be marginal ($T_{m,pure}$ - $Tm_{,modified}$ < 10°C), indicating that the molecular architecture of PET remains largely unaffected by these chain extenders. This phenomenon can be attributed to the limited perturbation of the crystalline domains despite the introduction of chain extension moieties.

3.2 Non-isothermal crystallization kinetics

3.2.1 Crystallization behavior under dynamic conditions

The non-isothermal crystallization behavior of E12, E20, E44, E51 modified PET and pure PET samples was systematically investigated through differential scanning calorimetry (DSC) analysis, with Figures 2a–e presenting their respective cooling crystallization curves obtained at different cooling rates ranging from 5°C to 20°C/min, while Table 4 quantitatively summarizes the corresponding kinetic parameters including crystallization peak temperature (Tp), crystallization enthalpy (ΔHc). The experimental results clearly demonstrate two significant trends: firstly, all samples exhibit a progressive shift of crystallization peak temperature (Tp) toward lower temperature regions with increasing cooling rates, showing an average depression of 12°C–18°C across the studied cooling rate range, which can be attributed to the enhanced supercooling effect (ΔT = Tm - Tc) that requires lower temperatures to overcome the nucleation energy barrier under faster cooling conditions; secondly, the crystallization enthalpy (ΔHc) displays a positive correlation with cooling rate, which results from the competition between two opposing factors - the increased nucleation density at higher supercooling that promotes crystallization and the restricted molecular chain mobility that hinders complete crystal formation. This phenomenon can be fundamentally explained by considering the crystallization kinetics: at higher cooling rates, the polymer system undergoes a more rapid transition from a high-temperature state where molecular chains possess sufficient mobility for rearrangement to a low-temperature state where chain movement becomes severely restricted, thereby preventing the molecular chains from achieving optimal orientation and regular arrangement within the crystal lattice within the available time frame. Particularly noteworthy is the observation that modified PET samples exhibit approximately 30% greater variation in crystallization enthalpy compared to pure PET across the same cooling rate range, indicating that the chain extension modification significantly enhances the material's sensitivity to cooling conditions, which may be attributed to the introduction of additional constraints on molecular mobility through the formation of branched or crosslinked structures during the modification process, consequently making the crystallization behavior more dependent on processing conditions and providing important implications for industrial processing parameter optimization of modified PET materials.

3.2.2 Ozawa crystallization kinetics analysis

The Ozawa formalism, which extends Avrami theory to non-isothermal conditions by incorporating cooling rate (R) dependence, was employed to analyze the crystallization kinetics, as shown in Equations 1, 2:

$$1 - Xc = \exp\left[-K_T / R^m\right] \tag{1}$$

$$\lg\left[-\ln\left(1 - Xc\right)\right] = \lg K_T - m \lg R \tag{2}$$

where Xc is the relative crystallinity at temperature T, R is the cooling rate, m is the Ozawa index, K_T is the Ozawa crystallization kinetic parameter, which is related to the nucleation method, nucleation rate, etc.

The non-isothermal crystallization behavior of pure PET and chain-extender modified PET systems was comprehensively investigated, with Figure 3 presenting their crystallization curves obtained at a controlled cooling rate of 15°C/min. The comparative analysis reveals that all modified PET samples exhibit systematically lower characteristic crystallization temperatures (initial crystallization temperature T0, final crystallization temperature Tf, and crystallization peak temperature Tp) compared to pure PET, with the depression magnitude varying between 5°C–12°C depending on the chain extender type. This temperature depression phenomenon, particularly the reduction in T0 which serves as an indicator of nucleation kinetics (Qureshi et al., 2000),

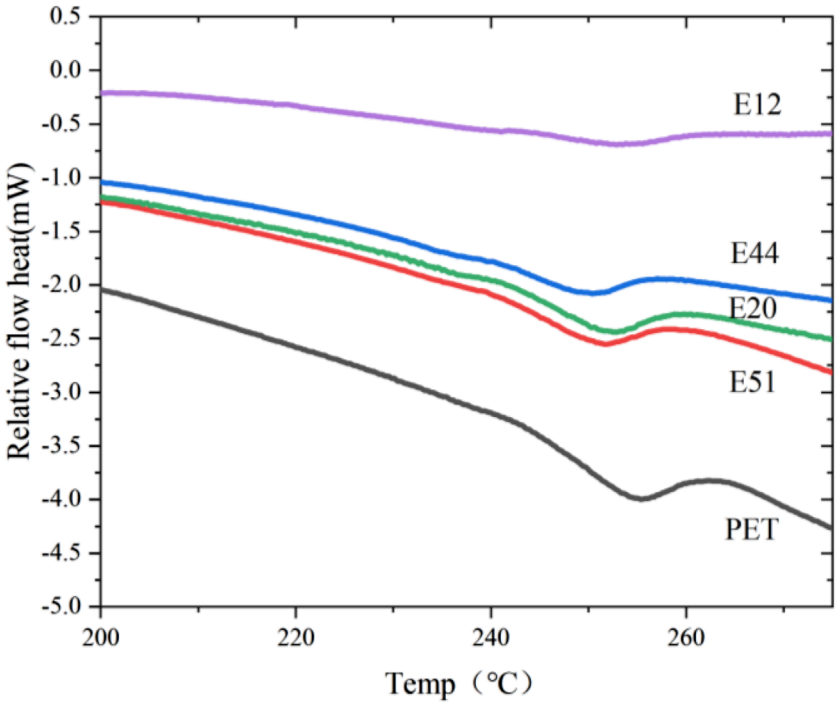

FIGURE 1
DSC curve after 190°C isothermal crystallization.

TABLE 3 Characteristic temperature in DSC curve.

Sample	E12	E20	E44	E51	纯PET
Peak temperature of heating curve/°C	252.8923	252.8288	250.3699	251.7591	255.3446
Melting point/°C	261.0387	259.2596	256.7359	259.0376	262.7054

suggests that the chain extension modification significantly retards the nucleation process and prolongs the overall crystallization duration, likely due to the introduced topological constraints that hinder molecular chain mobility and reorganization.

Further insights into the crystallization kinetics were obtained from the relative crystallinity (Xc) versus temperature profiles shown in Figures 4a–e, where all samples display characteristic sigmoidal curves indicative of three distinct crystallization stages: an initial induction period with minimal crystallinity development corresponding to nucleation establishment, followed by a rapid growth phase where crystallinity increases sharply as spherulites expand until impingement occurs, and finally reaching a plateau region where crystal growth continues at a diminishing rate until reaching equilibrium (Sekelik et al., 1999). The transformation of these temperature-dependent profiles into time-dependent crystallization curves maintains the sigmoidal shape due to the linear temperature-time relationship inherent in non-isothermal crystallization.

In the context of scientific investigations and data - driven analyses, a well - established and effective approach is to explore the relationship between two key variables, namely $\lg[-\ln(1-Xc)]$ and $\lg R$. This exploration often involves the construction of a linear model, which can provide valuable insights into the underlying mechanisms governing their interaction.

Specifically, when we carefully selects the data points corresponding to $\lg[-\ln(1-Xc)]$ and $\lg R$ and connects them by drawing a straight line, this graphical representation serves as a powerful tool for extracting meaningful information. The slope of this straight line is a parameter of great significance, known as the Ozawa index m.

The crystallization mechanism was further examined through Ozawa analysis as presented in Figure 5, where deviations from ideal linearity in the $\lg[-\ln(1-Xc)]$ versus lgR plots were observed for all samples, with modified PET systems showing more pronounced non-linearity than pure PET. These deviations primarily stem from two factors: the occurrence of secondary crystallization processes not accounted for in the Ozawa model, and the varying crystallization rates at different stages of the transformation. Notably, the linearity quality varies significantly among different modified PET systems - E12, E20 and E44 modified PETs demonstrate relatively better linear correlations suggesting limited secondary crystallization, while E51 modified PET exhibits

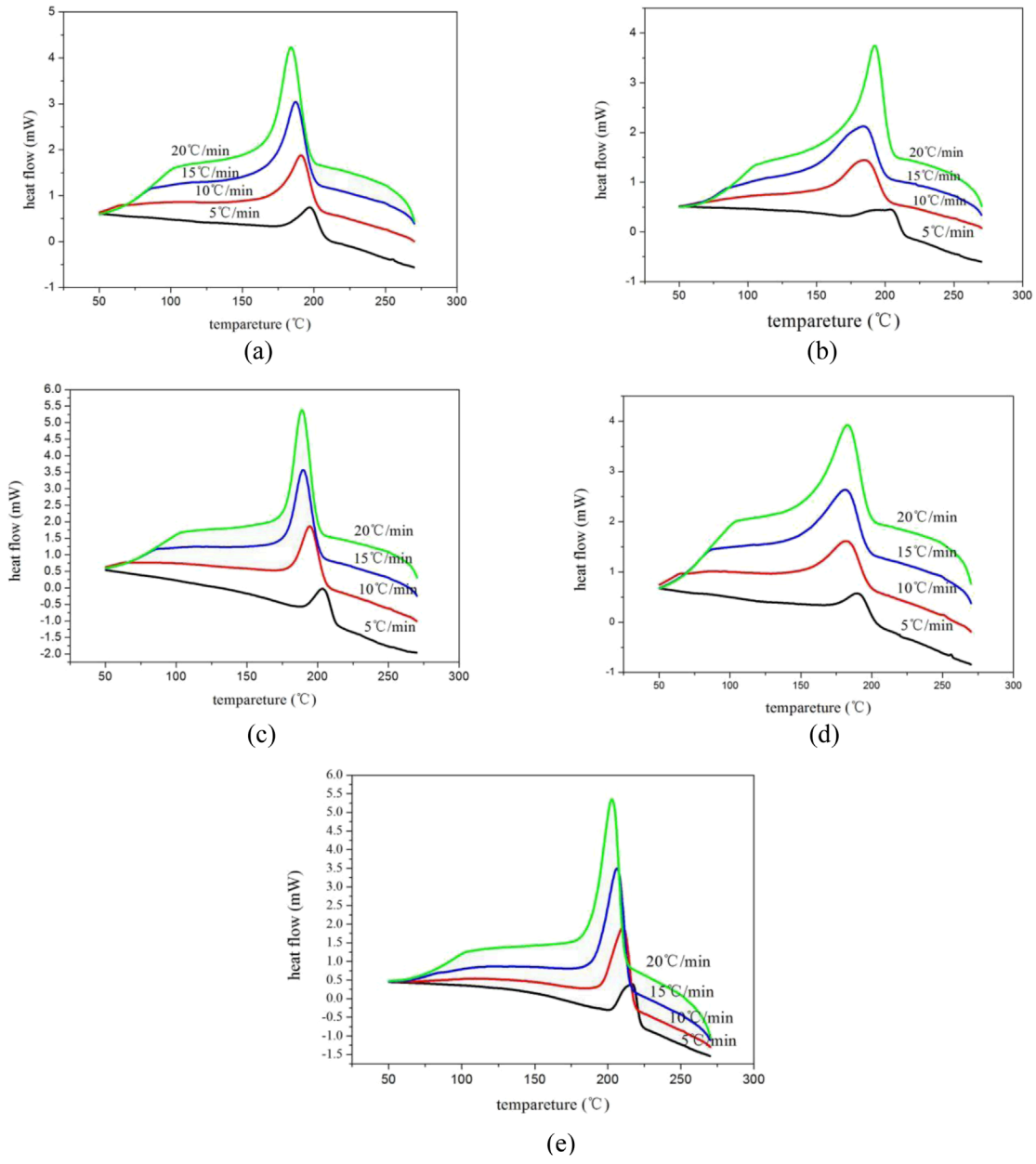

FIGURE 2
Cooling curves of modified PET at different cooling rates. **(a)** E12 **(b)** E20 **(c)** E44 **(d)** E51 **(e)** Pure PET.

the poorest linear relationship indicating substantial secondary crystallization. These differences likely originate from variations in chain extender reactivity and the resulting polymer architecture, where E51 modification may introduce more pronounced branching or crosslinking that promotes subsequent crystallization processes after the primary crystallization event. The comprehensive analysis suggests that while chain extension modification generally retards primary crystallization kinetics, the specific effects on secondary crystallization behavior are strongly dependent on the chain extender chemistry, with important implications for material processing and final properties.

3.2.3 Study on non - isothermal crystallization kinetics by Jeziorny method

The crystallization behavior of polymers is a complex and crucial phenomenon that significantly influences their physical and mechanical properties. In reality, the actual crystallization process of polymers is highly intricate, involving a multitude of factors such as molecular chain mobility, temperature gradients, and the presence of impurities. While the Avrami isothermal crystallization equation has long been a cornerstone in the study of polymer crystallization, it provides only a theoretical framework that is based on the assumption of isothermal conditions. In practical scenarios,

TABLE 4 Non-isothermal kinetic parameters of Modified PET.

Example	R/(°C·min^{-1})	T_0/°C	T_f/°C	T_p/°C	ΔHc/(J·g^{-1})
E12	5	211.04	167.67	197.36	10.8757
	10	205.80	147.77	191.21	22.9166
	15	204.45	140.31	187.22	35.8354
	20	201.81	140.17	184.07	46.4884
E20	5	215.61	170.59	204.52	10.3952
	10	205.82	150.01	185.62	20.3262
	15	204.79	142.19	184.46	30.2437
	20	208.78	143.35	192.44	48.6487
E44	5	217.32	182.06	203.89	12.9241
	10	209.85	172.25	194.70	24.5846
	15	207.08	156.09	189.94	40.5720
	20	205.53	156.17	188.96	53.7594
E51	5	207.32	166.38	191.26	9.2604
	10	203.61	131.73	182.91	26.0538
	15	203.52	134.23	181.79	35.8548
	20	203.32	136.88	183.20	49.2359
Pure PET	5	225.66	192.55	216.83	13.6901
	10	220.39	183.52	210.45	28.4673
	15	218.65	180.11	206.40	44.5919
	20	214.70	176.08	203.02	61.9033

Note: T_0 is the initial crystallization temperature of the sample; T_f is the final crystallization temperature of the sample; T_p is the peak crystallization temperature of the sample.

polymers often undergo non - isothermal crystallization, where the temperature changes continuously during the process.

To address this discrepancy and better understand non - isothermal crystallization, Jeziorny proposed the Jeziorny non - isothermal crystallization equation, which builds upon the foundation of isothermal crystallization. This approach simplifies the non - isothermal crystallization process by regarding it as a series of isothermal crystallization steps. The classic Avrami equation (Frounchi and Dourbash, 2009), which serves as the basis for the Jeziorny equation, as shown in Equations 3, 4:

$$1 - Xc = \exp\left(-Z_t t^n\right) \tag{3}$$

$$\ln\left[-\ln\left(1 - Xc\right)\right] = \ln Z_t + n \ln t \tag{4}$$

here, Xc represents the relative crystallinity corresponding to time t, Z_t is the crystallization rate constant, and n is the Avrami index. The Avrami index n is related to the nucleation mechanism and the growth geometry of the polymer crystals. A value of n = 1 typically indicates one - dimensional crystal growth, n = 2 for two - dimensional growth, and n = 3 for three - dimensional growth.

In the Jeziorny equation, Z_t is initially considered a constant. However, in non - isothermal crystallization, the rate constant should account for the temperature change that occurs throughout the process. Therefore, Z_t needs to be corrected. The corrected value is $\lg Z_c = \lg Z_t/R$, where R is the cooling rate. This correction factor is essential because the cooling rate has a profound impact on the crystallization rate and the final crystal structure of the polymer. A higher cooling rate can lead to smaller crystal sizes and a more disordered structure, while a lower cooling rate allows for more time for crystal growth and results in larger and more perfect crystals.

In the non - isothermal crystallization process, the relationship between time t and temperature T can be expressed as $t = (T_0 - T)/R$, where T_0 represents the crystallization starting temperature, and T represents the temperature at time t. By plotting $\ln[-\ln(1 - Xc)]$ against $\ln t$ (as shown in Figure 6), we can analyze the crystallization kinetics. From the figure, it is evident that at

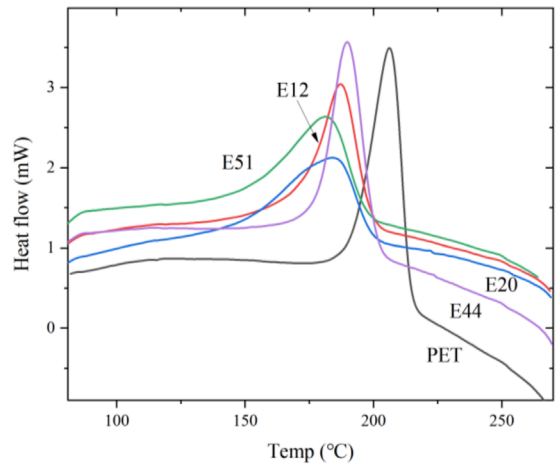

FIGURE 3
Cooling crystallization curve of modified PET at 15°C/min.

any given temperature, the initial part of the curve exhibits a good linear relationship. This linear region corresponds to the primary crystallization stage, where the polymer chains start to align and form crystal nuclei, followed by the growth of these nuclei.

However, the latter part of the curve shows different degrees of turning points. It is generally accepted that these turning points are caused by the secondary crystallization process that occurs in the later stage of polymer crystallization. Secondary crystallization involves the filling of defects and the thickening of existing crystals. Unfortunately, the Avrami equation does not take this secondary crystallization process into account. As a result, there are significant limitations when using the Avrami equation to analyze data obtained from non - isothermal crystallization experiments. This highlights the need for more advanced models or modified equations that can accurately describe the entire non - isothermal crystallization process, including both primary and secondary crystallization stages, to gain a more comprehensive understanding of polymer crystallization kinetics.

Table 5 presents the Jeziorny non - isothermal crystallization kinetic parameters, with a particular focus on the Avrami index *n*. The Avrami index is a crucial parameter in the study of crystallization kinetics as it provides insights into the mechanism of the crystallization process. By analyzing the data in Table 5, we can explore the influence of cooling rate and the addition of chain extenders on the crystallization behavior of poly (ethylene terephthalate) (PET).

When examining the effect of cooling rate on the Avrami index *n* for both modified PET and pure PET, it is evident that the change in cooling rate has a negligible impact on the *n* values. This observation implies that the mechanism of crystallization kinetics remains relatively stable regardless of the cooling rate. Crystallization kinetics is a complex process influenced by various factors, and the fact that the cooling rate does not significantly alter the *n* values suggests that the fundamental crystallization mechanism is not directly related to the cooling rate, as supported by previous research.

To further understand the impact of chain extenders on the crystallization mechanism, we compare the average *n* values of different types of modified PET (E12, E20, E44, and E50) and pure PET. The average *n* values for E12, E20, E44, and E50 modified PET are 2.5352, 2.5496, 2.9912, and 2.6313 respectively, while that of pure PET is 2.7576. The similarity among these values indicates that the addition of these specific types of chain extenders does not change the crystallization mechanism of PET. The crystallization mechanism is mainly determined by the molecular structure and intermolecular forces of the polymer, and the chain extenders do not disrupt the inherent crystallization mode of PET.

Another important aspect of non - isothermal crystallization kinetics is the corrected crystallization rate constant Z_c and the half - crystallization time $t_{1/2}$. The corrected Z_c shows an increasing trend with the increase of cooling rate. This increase in Z_c implies that a higher cooling rate promotes the crystallization process, as a larger Z_c value indicates a faster crystallization rate. Correspondingly, the half - crystallization time $t_{1/2}$ decreases as the cooling rate increases. The half - crystallization time represents the time required for the polymer to reach 50% of its final crystallinity. A shorter $t_{1/2}$ at higher cooling rates clearly demonstrates that an increase in cooling rate is beneficial for accelerating the crystallization of PET, which is consistent with the findings of previous studies.

However, when comparing the half - crystallization time of chain - extended modified PET and pure PET at any given cooling rate, we find that the half - crystallization time of chain - extended modified PET is consistently greater than that of pure PET. This result suggests that the addition of these types of chain extenders has a negative effect on the crystallization process of PET. The chain extenders may increase the molecular weight and entanglement of the polymer chains, making it more difficult for the polymer chains to arrange themselves into an ordered crystalline structure. As a result, the crystallization ability of PET is reduced, and the time required to reach a certain degree of crystallinity is prolonged.

In conclusion, the non - isothermal crystallization kinetics of PET is affected by both cooling rate and the addition of chain extenders. The crystallization mechanism, as reflected by the Avrami index *n*, is independent of the cooling rate and is not significantly changed by the addition of the studied chain extenders. An increase in cooling rate accelerates the crystallization of PET, but the addition of chain extenders inhibits the crystallization process and reduces the crystallization ability of PET. These findings provide valuable insights for the design and processing of PET - based materials, as understanding the crystallization behavior is crucial for controlling the final properties of the materials. Future research could focus on exploring different types of chain extenders or modifying the processing conditions to optimize the crystallization behavior of PET.

3.2.4 Mo method non - isothermal crystallization kinetics study

In the realm of polymer science, accurately understanding the crystallization kinetics is of utmost importance as it significantly influences the final properties and performance of polymer materials. The Avrami equation, a well - established theoretical framework, is commonly employed to describe the static isothermal crystallization process under ideal conditions. Under ideal isothermal circumstances, the polymer chains have sufficient time

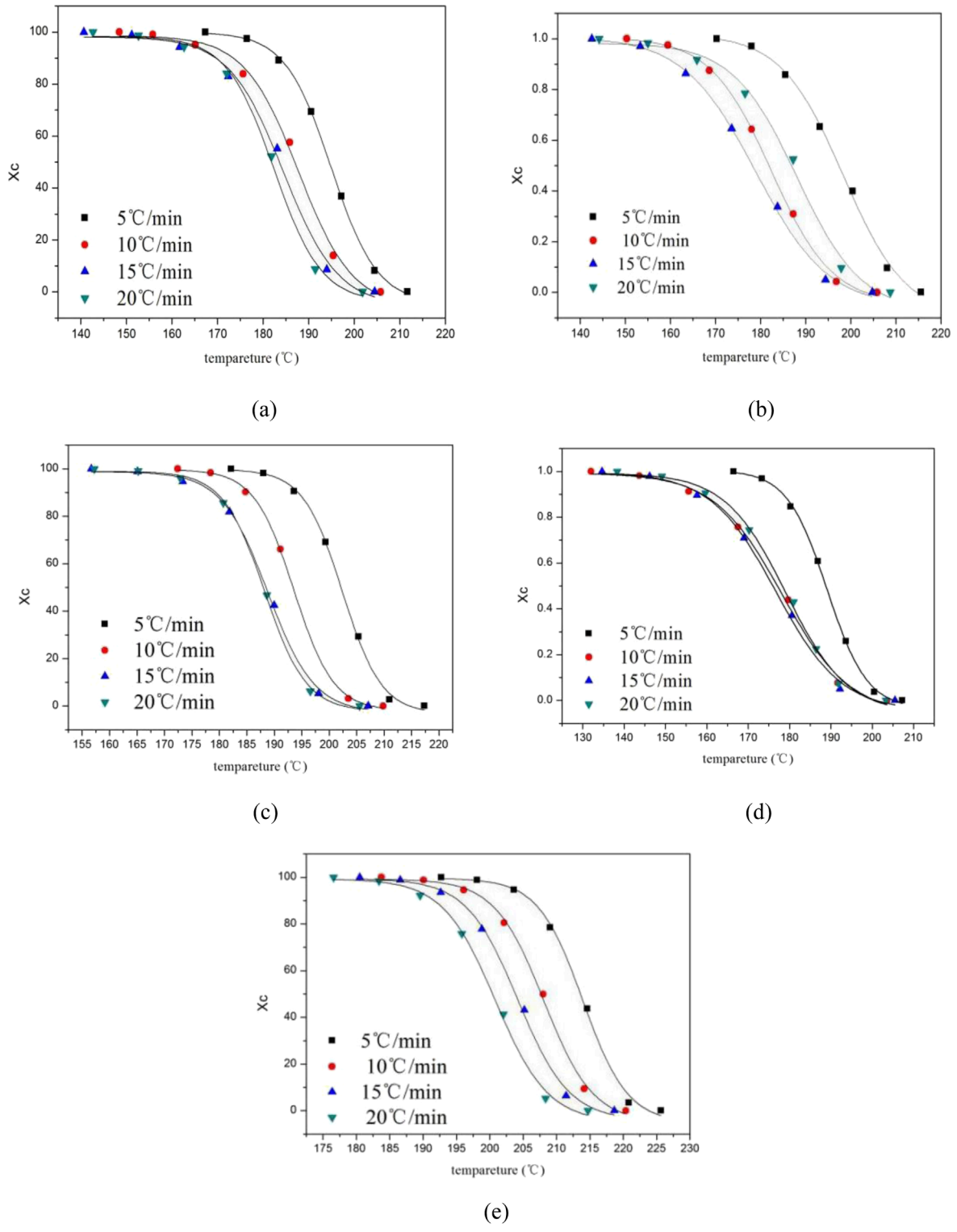

FIGURE 4
Relation curve between temperature and relative crystallinity Xc of modified PET. **(a)** E12 **(b)** E20 **(c)** E44 **(d)** E51 **(e)** Pure PET.

and a stable thermal environment to arrange themselves into ordered crystalline structures. The Avrami equation is based on the fundamental principles of nucleation and growth kinetics, which can effectively characterize this relatively simple and stable crystallization process. However, in real - world scenarios, the crystallization process of polymers is far more complex and dynamic. It typically occurs under non - isothermal conditions, where the temperature changes continuously over time. This

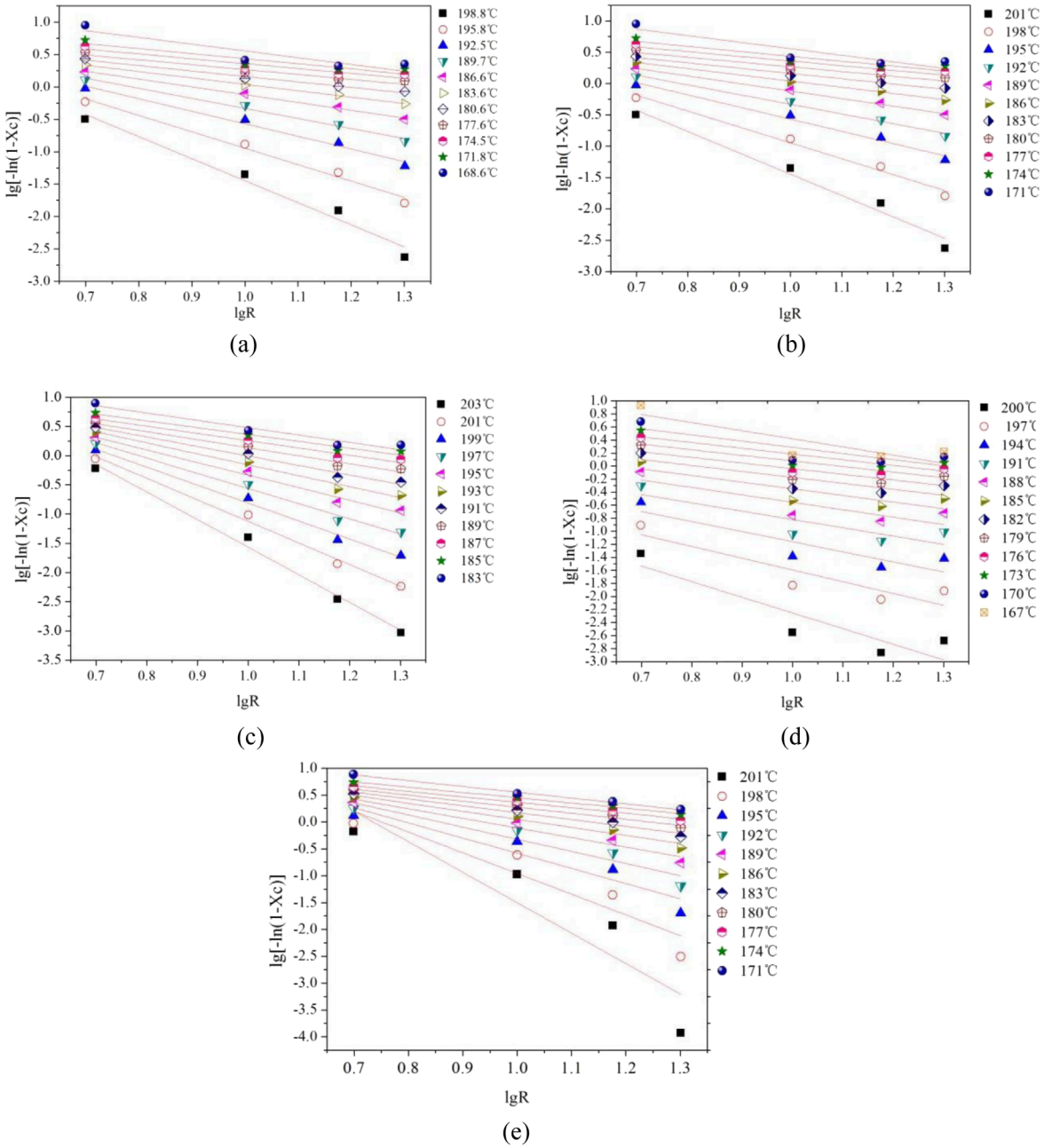

FIGURE 5
The relationship curve of modified PET -lgR. **(a)** E12 **(b)** E20 **(c)** E44**(d)** E51 **(e)** Pure PET.

dynamic nature of the crystallization process introduces additional factors that the Avrami equation fails to account for. For instance, the varying temperature affects the mobility of polymer chains, the rate of nucleation, and the growth of crystals. As a result, the Avrami equation exhibits certain limitations in accurately depicting the actual crystallization process of polymers.

To address the non - isothermal crystallization behavior, the Ozawa equation was proposed. This equation takes into consideration the non - isothermal crystallization of crystals from the perspectives of crystal nucleation and growth. It attempts to describe how the crystallization process proceeds under non - isothermal conditions by considering the influence of cooling rate on nucleation and growth. Nevertheless, the Ozawa equation also has its drawbacks. One of the major limitations is that it does not consider the secondary crystallization phenomenon that often occurs during the crystallization process. Secondary crystallization refers to the further crystallization that takes place after the primary crystallization, which can significantly affect the final degree of crystallinity and the physical properties of the polymer. Moreover, different cooling rates lead to different crystallization temperature ranges for the material. This variation in the crystallization temperature range causes the linear relationship

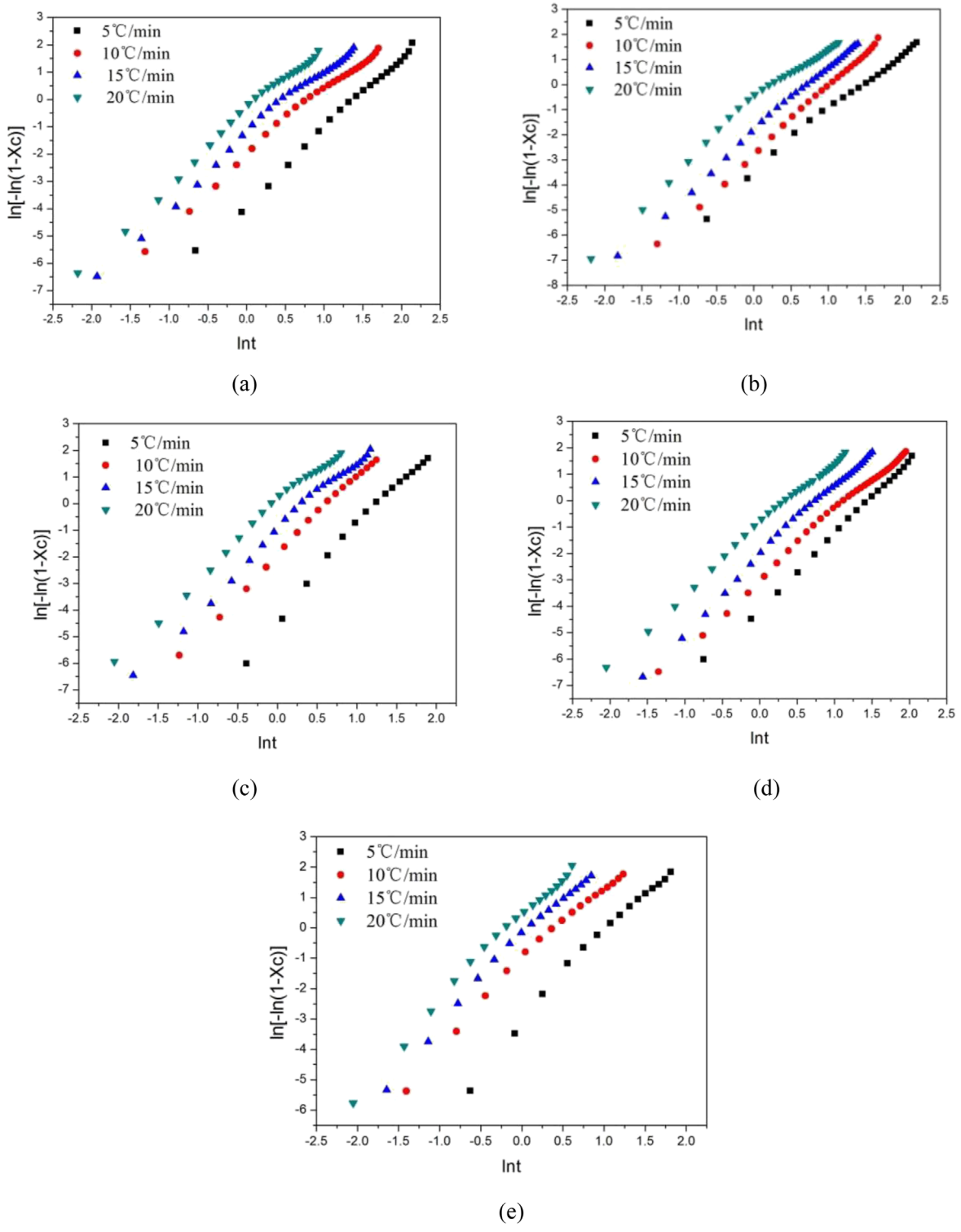

FIGURE 6
Relation curve of modified PET -lnR. **(a)** E12 **(b)** E20 **(c)** E44 **(d)** E51 **(e)** Pure PET.

assumed in the Ozawa equation to become unclear. Consequently, the Ozawa equation is unable to provide a comprehensive and accurate description of the crystallization process of crystals.

In response to these limitations, Mo proposed an innovative approach by combining the Avrami equation and the Ozawa equation. Through this combination, they

10.3389/fmats.2025.1619133

TABLE 5 Kinetics parameters of Jeziorny non-isothermal crystallization.

Example	R/(°C/min)	n	lnZ_t	Z_c	$t_{1/2}$/min
E12	5	2.6772	−3.79655	0.467989228	3.268
	10	2.3692	−2.08688	0.81164843	1.820
	15	2.4762	−1.41808	0.909792555	1.344
	20	2.6182	−0.518	0.974432528	0.978
E20	5	2.3419	−3.44098	0.502481729	3.630
	10	2.7333	−2.8057	0.755353067	2.349
	15	2.6390	−1.94026	0.878665793	1.767
	20	2.4841	−0.86744	0.957555113	1.025
E44	5	3.3213	−4.30395	0.422827916	2.944
	10	3.0142	−1.94531	0.823220658	1.625
	15	2.8454	−1.15513	0.925881829	1.198
	20	2.7837	−0.0767	0.996172344	0.865
E51	5	2.7887	−4.06152	0.443834293	3.652
	10	2.5015	−2.96281	0.743578453	2.590
	15	2.7188	−2.15201	0.8663491	1.787
	20	2.5163	−0.99059	0.951677083	1.216
Pure PET	5	2.8385	−3.09428	0.538560198	2.372
	10	2.6012	−1.20892	0.886129656	1.220
	15	2.7691	−3.9065	0.770717536	0.980
	20	2.8216	0.3669	1.018514303	0.697

derived the Mo non - isothermal crystallization kinetics equation:

$$\lg R = \lg F(T) - a \lg t$$

where R represents the cooling rate. n is the Avrami index, which reflects the nucleation and growth mechanism in the Avrami equation, and m is the Ozawa index, which is related to the influence of the cooling rate on crystallization in the Ozawa equation. $F(T) = \left(K_T/Z_t\right)^{\frac{1}{m}}$, $F(T)$ represents the cooling rate value that must be selected when the measured system reaches a certain degree of crystallinity at the crystallization time T. It serves as a crucial parameter in the Mo equation, linking the cooling rate, crystallization time, and degree of crystallinity.

To further analyze the data obtained from the Mo equation, a fitting straight line is constructed between lg R and lg t, as shown in Figure 7. The intercept $F(T)$ of this curve is a key indicator of the crystallization speed. According to the established relationship, a larger intercept value of $F(T)$ corresponds to a slower crystallization rate. By carefully examining Figure 7, it is evident that the linear relationship between the results obtained from the Mo method under the selected crystallinity is more pronounced compared to that of the Ozawa equation. This enhanced linearity indicates that the Mo equation is more effective in describing the crystallization behavior of these modified polyethylene terephthalate (PET) materials.

Table 6 presents the Mo crystallization kinetic parameters, which provide valuable insights into the crystallization characteristics of different PET samples. From the data in the table, it can be observed that the $F(T)$ value of pure PET is smaller than that of modified PET. This difference in $F(T)$ values further confirms that the crystallization rate of these chain - extended modified PETs is slower than that of pure PET. Through a detailed comparison, it is found that the E44 modified PET has a relatively smaller impact on the crystallization process. Additionally, there is a clear relationship between the relative crystallinity and the $F(T)$ value. As the relative crystallinity increases, the $F(T)$ value also increases. This trend implies that an increase in the

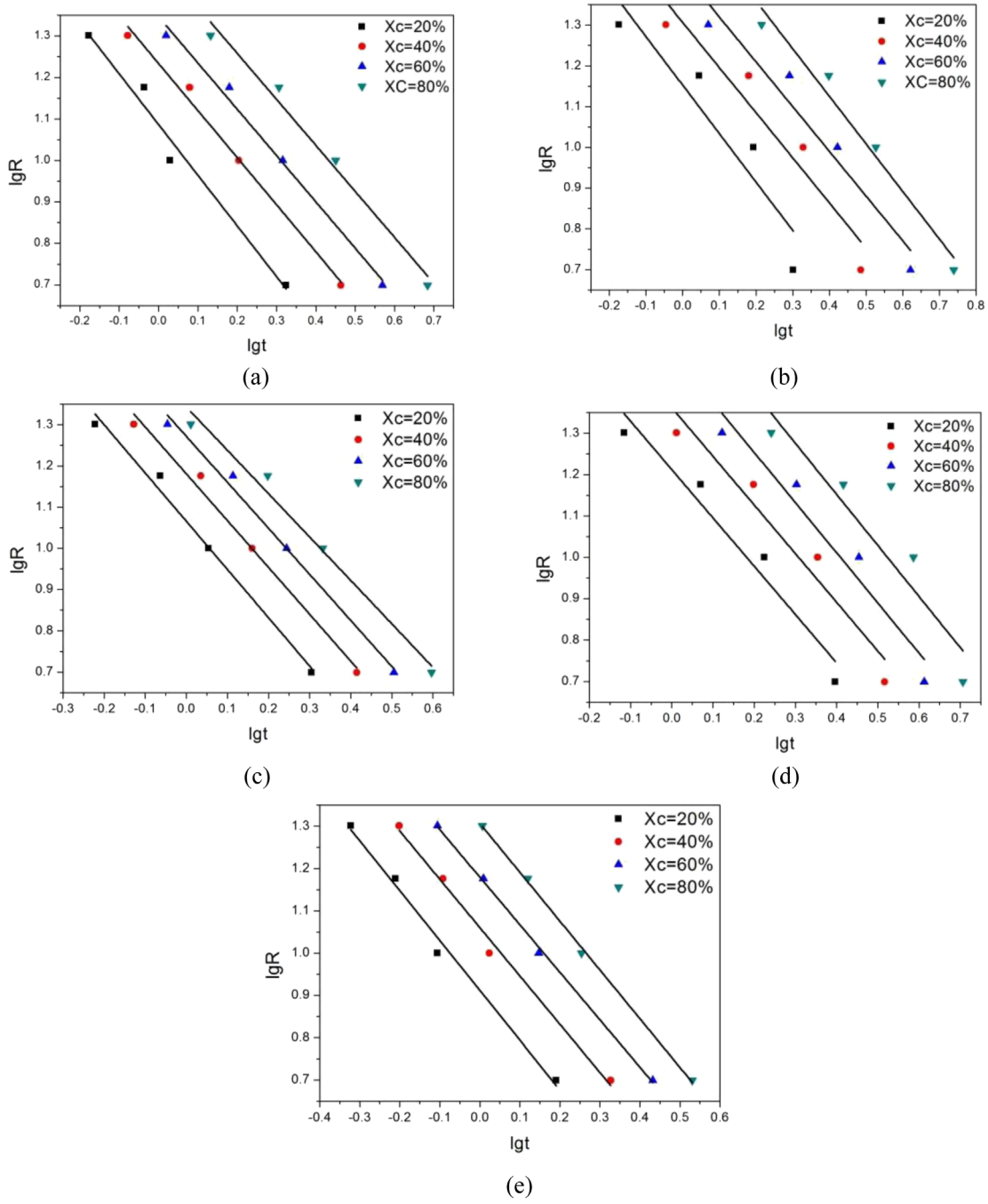

FIGURE 7
lg(R)-lgt relationship curve of modified PET. **(a)** E12 **(b)** E20 **(c)** E44 **(d)** E51 **(e)** Pure PET.

cooling rate is beneficial for PET to achieve a higher crystallinity per unit time.

In conclusion, the Mo non - isothermal crystallization kinetics equation offers a more accurate and comprehensive description of the crystallization process of modified PET materials compared to the Avrami and Ozawa equations. It effectively overcomes the limitations of the previous equations by integrating their advantages.

One notable aspect of these modified PET materials is their environmental advantages. PET is a widely - used thermoplastic polymer, and the modified PET in this study shows enhanced recyclability. During the recycling process, the modified structure allows for easier depolymerization and repolymerization, reducing the energy consumption and waste generation associated with traditional PET recycling. Moreover, compared to some other polymers, the raw materials for modified PET can be sourced more sustainably. For example, it can utilize a certain proportion of bio - based monomers, which helps to decrease the reliance on fossil - based resources and lower the carbon footprint.

TABLE 6 Mo crystallization kinetics parameters.

Example	Kinetic parameters	Xc = 20%	Xc = 40%	Xc = 60%	Xc = 80%
E12	a	−1.04291	−1.3606	−0.95281	−1.10944
	lgF(T)	1.043	1.23383	1.28025	1.47996
E20	a	−1.19142	−1.1084	−1.09934	−1.16885
	lgF(T)	1.1529	1.30679	1.42978	1.59277
E44	a	−1.17063	−1.13569	−1.11694	−1.05253
	lgF(T)	1.06572	1.18086	1.27196	1.34316
E51	a	−1.16865	−1.17771	−1.21294	−1.23455
	lgF(T)	1.21221	1.36211	1.49609	1.64592
Pure PET	a	−1.17959	−1.1424	−1.12407	−1.1539
	lgF(T)	0.91186	1.06025	1.17956	1.30642

The analysis of the F(T) values and the linear relationships provides valuable information for understanding the crystallization behavior of different PET samples, which is crucial for optimizing the processing conditions and improving the performance of PET - based products. These improved PET products have a wide range of potential engineering applications. In the automotive industry, the enhanced mechanical properties of the modified PET make it suitable for manufacturing interior components such as dashboard panels and door trims. Its good heat resistance can also withstand the relatively high - temperature environment inside the vehicle. In the aerospace field, the lightweight yet strong nature of the modified PET can be used to fabricate non - structural parts, reducing the overall weight of the aircraft and thus saving fuel consumption. In the construction industry, the modified PET can be made into pipes and fittings. Its corrosion resistance ensures a longer service life, reducing the need for frequent replacements and maintenance.

Future research could further explore the application of the Mo equation in other polymer systems and investigate the influence of various factors on the crystallization kinetics based on this equation. This will not only expand the theoretical understanding of polymer crystallization but also open up new possibilities for the development of more environmentally - friendly and high - performance polymer materials in engineering applications.

4 Conclusion

In this study, the non-isothermal crystallization kinetics of pure PET and chain-extended modified PET were systematically investigated using Differential Scanning Calorimetry (DSC) under varying cooling rates. The Avrami, Ozawa, and Mo methods were applied to analyze the crystallization behavior, with particular emphasis on the Mo method as a more comprehensive approach for non-isothermal conditions. The *F(T)* parameter, derived from the Mo equation, was employed to quantitatively compare crystallization rates among different PET samples. Through experimental and theoretical analysis, the following conclusions were drawn:

1. The Mo equation successfully integrates the nucleation-growth mechanism (Avrami) and cooling-rate dependency (Ozawa), providing a more accurate description of non-isothermal crystallization kinetics.
2. Pure PET exhibits lower *F(T)* values than modified PET, indicating a faster crystallization rate due to unhindered chain mobility. Chain-extended PET modifications slow down crystallization, as evidenced by higher *F(T)* values, likely due to increased molecular weight and restricted chain rearrangement.
3. A positive correlation exists between *F(T)* and relative crystallinity: higher cooling rates promote faster crystallinity development per unit time.
4. Among the modified PET samples, E44 demonstrates the least impact on crystallization kinetics, suggesting it may be a favorable modifier for balancing enhanced mechanical properties and processability.

Data availability statement

The original contributions presented in the study are included in the article/supplementary material, further inquiries can be directed to the corresponding authors.

Author contributions

ML: Conceptualization, Writing – review and editing, Writing – original draft. MF: Investigation, Writing – review and editing, Writing – original draft, Software. WY: Project administration, Writing – review and editing, Writing – original draft, Methodology. PY: Supervision, Writing – review and editing, Software,

Writing – original draft. LF: Writing – review and editing. WJ: Writing – review and editing, Writing – original draft.

Funding

The author(s) declare that financial support was received for the research and/or publication of this article. This work was funded by Natural Science Foundation of Hunan Province [Grant No. S2024JJ7245 and 2023JJ50486]. We also appreciated Project Supported by Aid Program for Science and Technology Innovative Research Team in Higher Educational Institutions of Hunan Province; the Planned Science and Technology Project of Loudi City; Hunan Center of Technology Innovation for Advanced Ceramics; Hunan Province College Students' Innovation and Entrepreneurship Training Program Project.

Conflict of interest

Author WY was employed by Dofuoduo New Materials Co., Ltd.

The remaining authors declare that the research was conducted in the absence of any commercial or financial relationships that could be construed as a potential conflict of interest.

Generative AI statement

The author(s) declare that no Generative AI was used in the creation of this manuscript.

Publisher's note

References

Androsch, R., and Wunderlich, B. (2005). The link between rigid amorphous fraction and crystal perfection in cold-crystallized poly (ethylene terephthalate). *Polymer* 46 (26), 12556–12566. doi:10.1016/j.polymer.2005.10.099

Bian, J., Ye, S. R., and Feng, L. X. (2003). Heterogeneous nucleation on the crystallization poly (ethylene terephthalate). *J. Polym. Sci. Part B Polym. Phys.* 41 (18), 2135–2144. doi:10.1002/polb.10538

Billon, N. (2022). Development of order during strain induced crystallization of polymers, case of PET. *Polymer* 262, 125476. doi:10.1016/j.polymer.2022.125476

Calcagno, C. I., Mariani, C. M., Teixeira, S., and Mauler, R. (2007). The effect of organic modifier of the clay on morphology and crystallization properties of PET nanocomposites. *Polymer* 48 (4), 966–974. doi:10.1016/j.polymer.2006.12.044

Chaari, F., Chaouche, M., and Doucet, J. (2003). Crystallization of poly (ethylene terephthalate) under tensile strain: crystalline development versus mechanical behaviour. *Polymer* 44 (2), 473–479. doi:10.1016/s0032-3861(02)00739-5

Chen, X., Li, C., and Shao, W. (2007). Isothermal crystallization kinetics and melting behaviour of PET/ATO nanocomposites prepared by *in situ* polymerization. *Eur. Polym. J.* 43 (8), 3177–3186. doi:10.1016/j.eurpolymj.2007.04.042

Cruz-Delgado, V. J., Ávila-Orta, C. A., Espinoza-Martínez, A. B., Mata-Padilla, J. M., Solis-Rosales, S. G., Jalbout, A. F., et al. (2014). Carbon nanotube surface-induced crystallization of polyethylene terephthalate (PET). *Polymer* 55 (2), 642–650. doi:10.1016/j.polymer.2013.12.029

Dupaix, R. B., and Krishnan, D. (2006). A constitutive model for strain-induced crystallization in poly (ethylene terephthalate)(PET) during finite strain load-hold simulations. *J. Eng. Mater. Technol.* 128, 28–33. doi:10.1115/1.1924564

Flores, A., Pieruccini, M., Nöchel, U., Stribeck, N., and Calleja, F. B. (2008). Recrystallization studies on isotropic cold-crystallized PET: influence of heating rate. *Polymer* 49 (4), 965–973. doi:10.1016/j.polymer.2007.12.038

Frounchi, M., and Dourbash, A. (2009). Oxygen barrier properties of poly (ethylene terephthalate) nanocomposite films. *Macromol. Mater. Eng.* 294 (1), 68–74. doi:10.1002/mame.200800238

Gaonkar, A., Murudkar, V., and Deshpande, V. (2023). Isothermal crystallization, melting behavior and mechanical properties of polyethylene terephthalate (PET) and reorganized PET (RPET). *J. Macromol. Sci. Part B* 62 (3), 1–24. doi:10.1080/00222348.2023.2202927

Hanley, T. L., Forsythe, J. S., Sutton, D., Moad, G., Burford, R. P., and Knott, R. B. (2006). Crystallisation kinetics of novel branched poly (ethylene terephthalate): a small-angle X-ray scattering study. *Polym. Int.* 55 (12), 1435–1443. doi:10.1002/pi.2097

Ke, Y.-C., Wu, T.-B., and Xia, Y.-F. (2007). The nucleation, crystallization and dispersion behavior of PET–monodisperse SiO2 composites. *Polymer* 48 (11), 3324–3336. doi:10.1016/j.polymer.2007.03.059

Ke, Z., and Yongping, B. (2005). Improve the gas barrier property of PET film with montmorillonite by *in situ* interlayer polymerization. *Mater. Lett.* 59 (27), 3348–3351. doi:10.1016/j.matlet.2005.05.070

Lewis, E., Duckett, R., Ward, I., Fairclough, J., and Ryan, A. (2003). Retraction notice to: the barrier properties of polyethylene terephthalate to mixtures of oxygen, carbon dioxide and nitrogen. *Polymer* 44 (5), 1631–1640. doi:10.1016/s0032-3861(02)00933-3

Liangbin, L., Rui, H., Ling, Z., and Shiming, H. (2001). A new mechanism in the formation of PET extended-chain crystal. *Polymer* 42 (5), 2085–2089. doi:10.1016/s0032-3861(00)00387-6

Lu, X., and Hay, J. (2001). Isothermal crystallization kinetics and melting behaviour of poly (ethylene terephthalate). *Polymer* 42 (23), 9423–9431. doi:10.1016/s0032-3861(01)00502-x

Ou, C. F., Ho, M. T., and Lin, J. R. (2003). The nucleating effect of montmorillonite on crystallization of PET/montmorillonite nanocomposite. *J. Polym. Res.* 10 (2), 127–132. doi:10.1023/a:1024981914234

Piccarolo, S., Brucato, V., and Kiflie, Z. (2000). Non-isothermal crystallization kinetics of PET. *Polym. Eng. and Sci.* 40 (6), 1263–1272. doi:10.1002/pen.11254

Qureshi, N., Stepanov, E., Schiraldi, D., Hiltner, A., and Baer, E. (2000). Oxygen-barrier properties of oriented and heat-set poly (ethylene terephthalate). *J. Polym. Sci. Part B Polym. Phys.* 38 (13), 1679–1686. doi:10.1002/1099-0488(20000701)38:13<1679::aid-polb10>3.0.co;2-p

Sangroniz, L., van Drongelen, M., Cardinaels, R., Santamaria, A., Peters, G. W. M., and Müller, A. J. (2020). Effect of shear rate and pressure on the crystallization of PP nanocomposites and PP/PET polymer blend nanocomposites. *Polymer* 186, 121950. doi:10.1016/j.polymer.2019.121950

Saujanya, C., Imai, Y., and Tateyama, H. (2003). Structure development and isothermal crystallization behaviour of compatibilized PET/expandable fluorine mica hybrid nanocomposite. *Polym. Bull.* 51, 85–92. doi:10.1007/s00289-003-0197-1

Sekelik, D., Stepanov, E., Nazarenko, S., Schiraldi, D., Hiltner, A., and Baer, E. (1999). Oxygen barrier properties of crystallized and talc-filled poly (ethylene terephthalate). *J. Polym. Sci. Part B Polym. Phys.* 37 (8), 847–857. doi:10.1002/(sici)1099-0488(19990415)37:8<847::aid-polb10>3.3.co;2-v

Tan, S., Su, A., Li, W., and Zhou, E. (2000). New insight into melting and crystallization behavior in semicrystalline poly (ethylene terephthalate). *J. Polym. Sci. Part B Polym. Phys.* 38 (1), 53–60. doi:10.1002/(sici)1099-0488(20000101)38:1<53::aid-polb6>3.0.co;2-g

Tang, S., and Xin, Z. (2009). Structural effects of ionomers on the morphology, isothermal crystallization kinetics and melting behaviors of PET/ionomers. *Polymer* 50 (4), 1054–1061. doi:10.1016/j.polymer.2008.12.015

Wan, T., Chen, L., Chua, Y. C., and Lu, X. (2004). Crystalline morphology and isothermal crystallization kinetics of poly (ethylene terephthalate)/clay nanocomposites. *J. Appl. Polym. Sci.* 94 (4), 1381–1388. doi:10.1002/app.20975

Wang, Z.-G., Hsiao, B., Fu, B., Liu, L., Yeh, F., Sauer, B., et al. (2000). Correct determination of crystal lamellar thickness in semicrystalline poly (ethylene terephthalate) by small-angle X-ray scattering. *Polymer* 41 (5), 1791–1797. doi:10.1016/s0032-3861(99)00327-4

Wu, T., and Ke, Y. (2007). Melting, crystallization and optical behaviors of poly (ethylene terephthalate)-silica/polystyrene nanocomposite films. *Thin Solid Films* 515 (13), 5220–5226. doi:10.1016/j.tsf.2006.12.029

Zheng, H., and Wu, J. (2007). Preparation, crystallization, and spinnability of poly (ethylene terephthalate)/silica nanocomposites. *J. Appl. Polym. Sci.* 103 (4), 2564–2568. doi:10.1002/app.25132